




# Novel biogenic silver nanoparticles used for antibacterial effect and catalytic degradation of contaminants

T. My-Thao Nguyen<sup>1</sup> · T. Thanh-Tam Huynh<sup>2,3</sup> · Chi-Hien Dang<sup>3,4</sup> ·  
Dinh-Tri Mai<sup>3,4</sup> · T. Thuy-Nhung Nguyen<sup>5</sup> · Dinh-Truong Nguyen<sup>5</sup> ·  
Van-Su Dang<sup>6</sup> · Trinh-Duy Nguyen<sup>7</sup> · Thanh-Danh Nguyen<sup>2,3</sup> 

Received: 13 November 2019 / Accepted: 30 December 2019 / Published online: 6 January 2020  
© Springer Nature B.V. 2020

## Abstract

The study reports a versatile, cost-efficient and ecofriendly protocol for the synthesis of biogenic silver nanoparticles (AgNPs) using the aqueous extracts of Quao Binh Chau, *Stereospermum binhchauensis* and Che Vang, *Jasminum subtriplinerve* and their application in antibacterial activity and catalysis. The AgNPs with varying morphology and physical properties have been optimized using the absorption measurements. The biogenic AgNPs have been characterized by Fourier transform infrared spectroscopy, UV–Vis spectroscopy, transmission electron microscopy, X-ray diffraction analysis, energy-dispersive X-ray spectroscopy and thermal behaviors. Stable crystalline AgNPs with average particle sizes of 20.0 nm and 8.0 nm were fabricated from aqueous extract of Quao Binh Chau and Che Vang, respectively. The phytochemicals from the extracts involved in reduction and stabilization of AgNPs are identified by FTIR spectra and thermal gravimetric analysis. Both the biosynthesized AgNPs show the potent antibacterial activity against four tested bacterial strains including *Bacillus subtilis*, *Staphylococcus aureus*, *Escherichia coli* and *Agrobacterium tumefaciens*. High catalytic activity of the biogenic AgNPs in the degradation of toxic contaminants (4-nitrophenol and methyl orange) was observed. The antibacterial and catalytic activities are found to be size and phytochemical dependent. The antibacterial and catalytic activities of the biogenic nanoparticles would find applications in the biomedical and environmental fields.

**Keywords** Silver nanoparticles · *Stereospermum binhchauensis* · *Jasminum subtriplinerve* antibacterial agent · Catalysis · Pollutant degradation

**Electronic supplementary material** The online version of this article (<https://doi.org/10.1007/s11164-019-04075-w>) contains supplementary material, which is available to authorized users.

T. My-Thao Nguyen, T. Thanh-Tam Huynh these authors contributed equally to this study.

✉ Thanh-Danh Nguyen  
danh5463bd@yahoo.com; nguyenthandanh3@duytan.edu.vn

Extended author information available on the last page of the article

## Introduction

AgNPs have frequently considered in recent years due to wide application in various fields such as catalysis, energy science, environment, biomedicine, sensor and drug delivery [1–5]. Commonly, three principle factors are required for the synthesis of AgNPs, including solvent diluting silver ions, reductants and capping reagents. In spite of successful synthesis of AgNPs using chemical methods in good purity and well-defined nanoparticles, it is high cost with release of harmful products posing a high risk to the ecosystem [6–9]. As a result, it is necessary to investigate green approaches for the AgNPs synthesis which provides important advantages for the commercial applicability of the metallic nanoparticles in industrial products. The current trend using biological reducing resources such as enzyme, microbial and plant extracts has been reported frequently. Among all, aqueous extract of the plants as reducing and capping reagents was considered as an alternative to physicochemical synthesis due to simple procedure, cost-efficiency and friendly environmental operation at large scales [10–13]. For instant, Arunachalam et al. [14] fabricated AgNPs from *Coccinia grandis* leaf extract and efficient application for photocatalytic degradation of Coomassie Brilliant Blue G-250. Green synthesis of AgNPs using *Cynara cardunculus* and *Salvia microphylla* leaf extracts for antibacterial applications has been reported [15, 16]. Recently, AgNPs biosynthesized from *Forsythia suspensa* fruit induced damaging membrane integrity of the food-borne pathogens [17]. Reduction of silver ions into AgNPs using the plant extract has been attributed to the presence of active molecules in phytochemicals such as terpenoids, saccharides, proteins and polyphenols [18, 19]. Quao Binh Chau (*S. binhchaensis*) and Che Vang (*J. subtriplinerve*) are new species discovered in Vietnam [20, 21]. The antioxidant compounds such as triterpenoids, flavonoids and glucosides have been identified and reported in their phytochemicals which can be employed as reducing reagents in the green synthesis process of metallic nanoparticles [22–24].

Toxic pollutants cause many serious problems to human life and environment. With rapid development of industries, usage of toxic organic compounds such as dyes and pigments is unavoidable in various fields of science and technology. These compounds are non-biodegradable over time in industrial effluents. Therefore, it is critical to reduce and remove the pollutants from wastewater. Some of the techniques have reported for the treatment of the organic pollutants including adsorption [25], catalytic reduction [26, 27], photocatalytic degradation [28] and advanced oxidation processes [29]. Among them, catalytic degradation using nanometals has been widely employed for the treatment of wastewater due to its cost-efficiency and simply clean processing. Due to a large surface area, a high stability and dispersive nature in water, the biogenic nanocatalysts based on noble metals, e.g., silver, were widely investigated in literature [30]. In this work, we have described an effectively novel method for the biosynthesis of AgNPs utilizing the aqueous extract of Quao Binh Chau and Che Vang leaves as reducing and capping agents. The potential applicability of the biogenic AgNPs has been demonstrated by antibacterial activity and catalytic degradation of organic contaminants including 4-nitrophenol and methyl orange.

## Experimental

### Materials

Chemicals including  $\text{AgNO}_3$ ,  $\text{NaBH}_4$ , 4-nitrophenol (4-NP) and methyl orange (MO) were purchased from Acros Company (Belgium). Quao Binh Chau, *S. binhchauensis* and Che Vang, *J. subtripplinerve* were provided by Khai Minh Macrobionics (Ho Chi Minh city, Vietnam). Preparation of plant extracts was carried out as the previous report [31]. Briefly, dried powders of leaves (10 g) were refluxed with 100 mL of distilled water for 1 h. The mixture was filtered. The filtrate was stored in refrigerator (4 °C) for further studies.

### Optimization of AgNPs biosynthesis

The extracts were placed to  $\text{AgNO}_3$  solution under stirring in dark condition. Change in the color of solutions confirmed the formation of AgNPs. Reaction parameters including ratio of  $\text{AgNO}_3$  solution volume to extract volume (1, 5, 10, 15, 20, v/v), and the reaction time (0–200 min) were optimized through UV–Vis spectra from range of 200 to 600 nm. Reduction of silver ions induced increase of absorbance at the peaks of around 417 nm. For the following studies, the nanoparticles were biosynthesized in the optimized conditions. The solid AgNPs were obtained by centrifugation for 30 min at 4000 rpm and washed with water and then ethanol to remove silver ions and the impurities. Finally, the nanoparticles were dried in an oven at 90 °C overnight.

### Physicochemical characterization

Absorption spectra were measured by JASCO V-630 spectrophotometer. Fourier transform infrared (FTIR, Tensor 27 FTIR spectrophotometer, Bruker) was used to identify functional groups of organic compounds from the extracts and nanoparticles. X-ray diffraction (XRD) patterns of crystal AgNPs were determined on X-ray diffractometer Bruker, Model-D8 Advance. TEM and HRTEM (JEOL JEM2100) were utilized to analyze morphology and crystal structure of AgNPs. Chemical compositions were analyzed by using energy-dispersive X-ray (EDX) spectroscopy (EMAX ENERGY EX-400, Horiba). The particle size and zeta potential of the AgNPs solutions were measured by using nanoPartica, Horiba SZ-100 (Japan). Thermogravimetry (TG) analysis and different thermal analysis (DTA) were simultaneously measured on A LabSys evo S60/58988 Thermoanalyzer (Setaram, France) from 30 to 800 °C in the air atmosphere at a heating rate of 10 °C/min.

### Antibacterial activity

The procedure for the biotest was carried out via the disk diffusion method as previous report [31]. Four bacterial strains including *Bacillus subtilis*, *Staphylococcus aureus* (Gram-positive) and *Escherichia coli*, *Agrobacterium tumefaciens*

(Gram-negative) were used to study the antibacterial activity of biosynthesized AgNPs. Luria–Bertani broth and standard antibiotic ampicillin (0.01 mg/mL) were utilized as negative and positive control, respectively. Antibacterial activity was determined by diameters of inhibition zone (mm) around the paper disks. The extracts tested at volume of 10  $\mu$ L exhibited no activity with all bacterial strains.

### Catalytic activity

The catalytic activity of AgNPs was evaluated by reduction of 4-nitrophenol and methyl orange with excess amount of NaBH<sub>4</sub> at the room temperature. Briefly, aqueous solution of NaBH<sub>4</sub> (0.5 mL, 0.1 M) was added into pollutant solutions (2.5 mL, 0.1 mM) in the quartz cells. Then, AgNPs (1.0 mg) were added into the cell. The experiments of control samples without the catalyst were also carried out for corresponding pollutants. The reduction was evaluated by using UV–Vis spectrophotometers. Gradual decrease in absorbance of 4-NP and MO was observed at peaks of 400 and 464 nm, respectively. Evaluation of kinetics can be carried out by measurement of UV–Vis absorbance in a time-dependent manner [24]. Because this work used a very low concentration of the pollutants with respect to the borohydride concentration (120 excess of borohydride) and very low amount of AgNPs (1 mg), the degradation kinetics were considered as a pseudo-first-order reaction. The rate constant  $k$  can be calculated by the equation  $\ln(A_t/A_0) = -kt$ , where  $t$  is the reduction time,  $[A_0]$  is concentration of the pollutants at  $t=0$ , and  $[A_t]$  is concentration of the pollutants at time  $t$ .  $[A_t]$  can be determined from the absorption intensity of the maximum peaks of the corresponding pollutants. The value  $k$  can be calculated from the slope of straight line resulted by plots of  $\ln(A_t/A_0)$  vs reduction time.

## Results and discussion

### Biogenic synthesis

The active organic components of plant extracts are expected for green synthesis of AgNPs. A major advantage of a biogenic synthesis method such as that described in this work is the lack of toxic by reagents/products in the synthesis medium. In our strategy as illustrated in Fig. 1, leaves of two plants including Quao Binh Chau and Che Vang are used as stabilizing and reducing reagents for biogenic synthesis of QBC-AgNPs and CV-AgNPs, respectively. The dried leaves were refluxed with water for 1 h, and the yellow extract solutions were obtained after filtration process. Optimization of reducing conditions which can induce changes in shape, size and dispersion of the nanoparticles is particularly important for the reproduction [13, 24]. The reaction can be confirmed by color change which the colorless aqueous AgNO<sub>3</sub> solution became yellowish brown after the addition of leaf extracts. UV–Vis spectroscopy can be used to observe the formation of AgNPs. It is well known that surface plasmon resonance (SPR) vibration of the AgNPs is around 420–440 nm [32]. The biogenic AgNPs were characterized physicochemical properties and

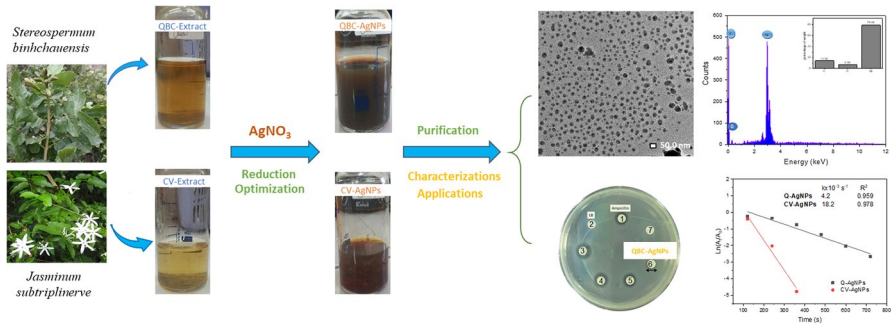


**Fig. 1** Schematic illustration of biogenic synthesis of QBC-AgNPs and CV-AgNPs

applied for evaluation of antibacterial activity and catalytic degradation of toxic compounds.

Two principle parameters including ratios of silver ions to extract (v/v) and reaction time were optimized by using UV–Vis spectroscopy. Changes in absorption intensity and  $\lambda_{max}$  values of SPR bands can provide essential insights into formation, size and morphology of the synthesized AgNPs. Plots of absorbance and  $\lambda_{max}$  values against the investigated parameters are described in Fig. 2. Different trends can be clearly observed for two aqueous extracts which can relate to their different phyto-components. Figure S1 shows that SPR peaks were not observed at low rates (1:1 and 5:1) for both biosynthesized AgNPs. Increase in ratios of silver ions to extract (10:1–20:1) induced various growing trends of colloidal solutions. A rapid increase of absorbance with constant  $\lambda_{max}$  values (around 440 nm) is observed for formation of QBC-AgNPs. It indicates no change in AgNPs morphology formed in the colloidal solution although the concentration of AgNPs is increasing with concentration of silver ions. Contrastingly, concentration of AgNPs reduced by Che Vang almost is not changed by growth of silver ion concentration. However, a significant red shift from 428 to 441 nm with silver ion concentrations is observed, indicating that the

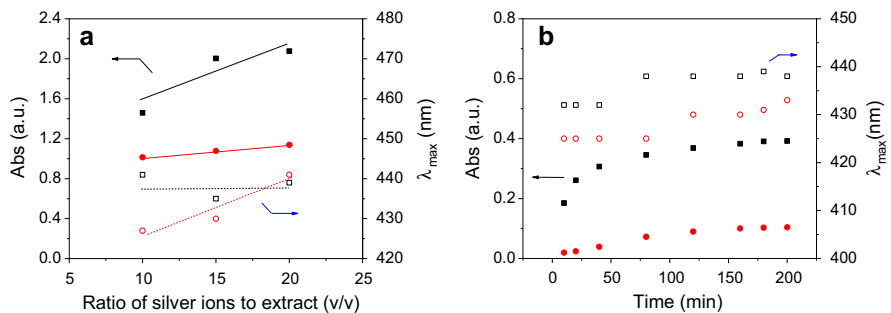


**Fig. 2** Plots of parameters versus absorbance (closed symbols) and wavelength (opened symbols) values: **a** Ratio of silver ion solution to extract and **b** reaction time for QBC-AgNPs (Square symbols) and CV-AgNPs (cycle symbols)

organic components presented Che Vang extract can induce a change in morphology of the synthesized nanoparticles. Interestingly, SPR bands of QBC-AgNPs (370–750 nm) are broader than that of CV-AgNPs (370–650 nm) as observed in UV–Vis spectra which can relate to difference in their morphology and size.

For optimization of reaction time, UV–Vis spectra of the reaction were measured for each regular time interval. No clear peaks of SPR band were found in initial 10 min for QBC-AgNPs and initial 40 min for CV-AgNPs. Both nanoparticles were rapidly formed and achieved a maximum absorbance value at 160 min with an insignificant change in maximum peaks (Fig. 2b). In summary, the optimum parameters including rate of 15:1 and stirring in 160 min are selected for further studies on characterization and application of both the biogenic AgNPs.

## Physicochemical characterizations of biosynthesized AgNPs

### FTIR analysis

FTIR analysis was carried out to determine the bioactive compounds present in the extracts responsible for reduction and stabilization of the biogenic AgNPs. The spectra of both the extracts were used as the references for analysis of the biogenic AgNPs. Slight shifts in percent transmittance of AgNPs spectra can be due to coordination of bioactive molecules with metal surface. The data are shown in Fig. 3. The peaks of Quao Binh Chau extract positioned at wave numbers 3421, 2920, 2852, 1616, 1437, 1385, 1264 and 1072  $\text{cm}^{-1}$  are, respectively, attributed to phytochemical compounds of polyphenols and amines, while these vibrations of Che Vang extract were observed at peaks 3418, 2923, 2873, 1632, 1430, 1260 and 1035  $\text{cm}^{-1}$ . The abroad vibrations at around 3420  $\text{cm}^{-1}$  relate to the phenolic hydroxyl groups, while the bands from 2920 and 2870  $\text{cm}^{-1}$  correspond to =C–H (arene). The bands from 1632 to 1451  $\text{cm}^{-1}$  are attributed to C=N and C=O stretching vibration of amide groups of protein. The peaks at 1070  $\text{cm}^{-1}$  might relate to C–OH of carboxylic acids [33, 34]. These characteristic vibrations of AgNPs biosynthesized by Quao Binh Chau and Che Vang leaf extracts are shifted to new bands at 3429, 2917, 2849, 1628, 1382, 1028  $\text{cm}^{-1}$  and 3421, 2916, 2848, 1625, 1383, 1064  $\text{cm}^{-1}$ , respectively. The strong peaks at 3429, 1628 and 1382  $\text{cm}^{-1}$  in the biogenic AgNPs revealed the presence of proteins and polyphenols which are responsible for reduction and stabilization of AgNPs. The peaks confirmed that the phytoconstituents play an essential role in formation and stabilization of AgNPs.

### Morphology

TEM micrographs were used to determine size and shape of AgNPs (Figs. 4 and 5). The results revealed difference between two the biosynthesized AgNPs. Figure 4a, b shows irregular shapes and heterogeneous population of QBC-AgNPs formed in a size range of 4–30 nm with an average value of 20 nm. This shape and distribution of nanoparticles may explain the broad bands observed in UV–Vis spectra, whereas a consistent distribution of CV-AgNPs is observed in range of 3–20 nm

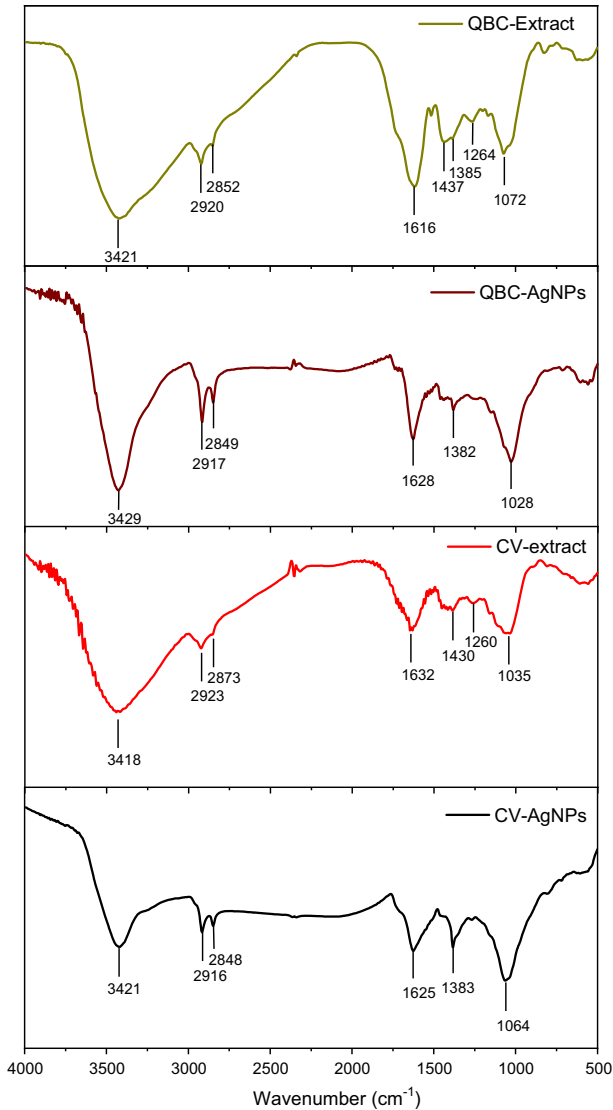


**Fig. 3** FTIR spectra of QBC extract, QBC-AgNPs, CV extract and CV-AgNPs

with an average size as low as 8 nm (Fig. 5a, b). As seen in TEM images, a light-colored outer covering surrounding the particles can correspond to the bioactive compounds as capping agents of nanoparticles present in the plant extracts. The various formations of AgNPs in both terms of morphology and size using the plant extract such as *A. squamosa* seeds and *L. Japonica* have been reported in literature [35–37]. The HRTEM micrographs of both the biosynthesized AgNPs show clear crystal lattice with lattice fringes of QBC-AgNPs and CV-AgNPs found to be 0.22 and 0.21 nm, respectively (Figs. 4c and 5c). It indicates growth of AgNPs taking

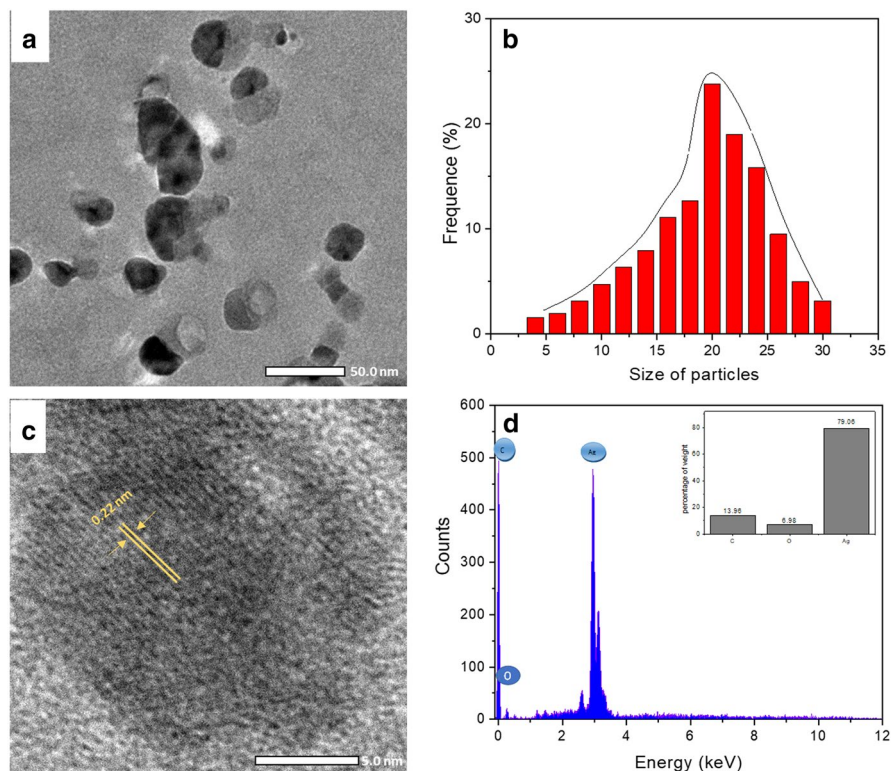


**Fig. 4** **a** TEM image; **b** particle size distribution; **c** HRTEM image and **d** EDX spectrum and average content of elements (inset) of QBC-AgNPs

place preferentially on the (111) plane [38, 39]. The elemental composition of the biosynthesized AgNPs was identified by EDX analysis (Figs. 4d and 5d). Appearance of strong signals around 3.0 keV in the spectra confirmed the nanoparticles formed from elemental silver [40, 41]. Average contents of silver in QBC-AgNPs and CV-AgNPs were found from EDX spectra data to be 79.06% (w/w) and 61.75% (w/w), respectively.

### XRD analysis

Crystal structure of biosynthesized AgNPs is determined using XRD analysis (Fig. 6). XRD patterns showed the Bragg's diffraction peaks at  $38.98^\circ$ ,  $43.12^\circ$  and  $63.82^\circ$  for Q-AgNPs and  $37.72^\circ$ ,  $44.02^\circ$  and  $64.08^\circ$  for CV-AgNPs corresponding to (111), (200) and (220) lattice planes, respectively, confirming the face centered cubic (fcc) crystal structure of AgNPs (Card No. 004-0783). The maximum intensity peak related to plane (111) confirmed lattice fringes in HRTEM micrograph. Small peaks observed in the XRD pattern can correspond to crystal AgCl and phytochemical compounds present in the leaf extracts [42].



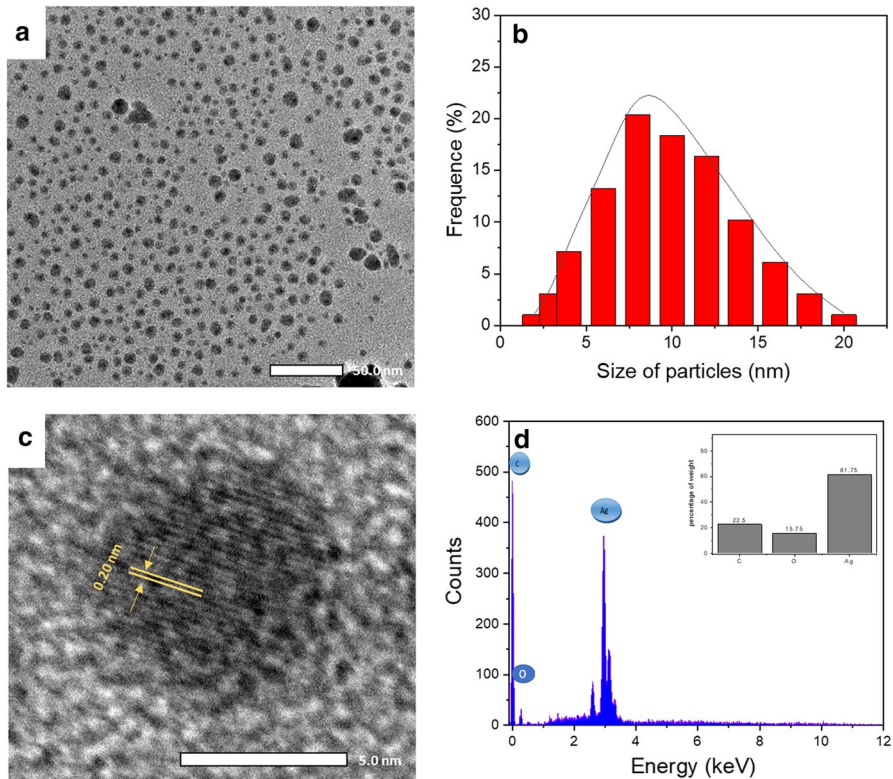


**Fig. 5** **a** TEM image; **b** particle size distributions; **c** HRTEM image and **d** EDX spectrum and average content of elements (inset) of CV-AgNPs

### Dynamic light scattering and zeta potential

For studying stability of the biosynthesized AgNPs, the zeta potential and size are measured using dynamic light scattering (DLS) at 25 °C as shown in Fig. 7. The zeta potential value of CV-AgNPs (−37.2 mV) colloidal solution is slightly higher than that of QBC-AgNPs (−31.5 mV), indicated the high stability of both nanoparticles in aqueous solution. The Vang-mediated AgNPs possessing high negative potential and small size of particles can relate to stabilization compounds present in its extract. The DLS measurements show broad size distribution in both the biosynthesized AgNPs. QBC-AgNPs are in ranging from 10 to 250 nm with a mean diameter of 81.7 nm (PI=0.69), while the hydrodynamic diameter of CV-AgNPs is in broad range with a mean size of 93.5 nm (PI=0.66). DLS measurements indicate much higher hydrodynamic diameters than the sizes found in the TEM micrographs due to the two techniques measuring different properties which has been explained elsewhere [43]. The DLS diameters would measure the whole particles including core and capping agents, while the TEM images would only provide size of the silver core.

**Fig. 6** XRD patterns of QBC-AgNPs and CV-AgNPs

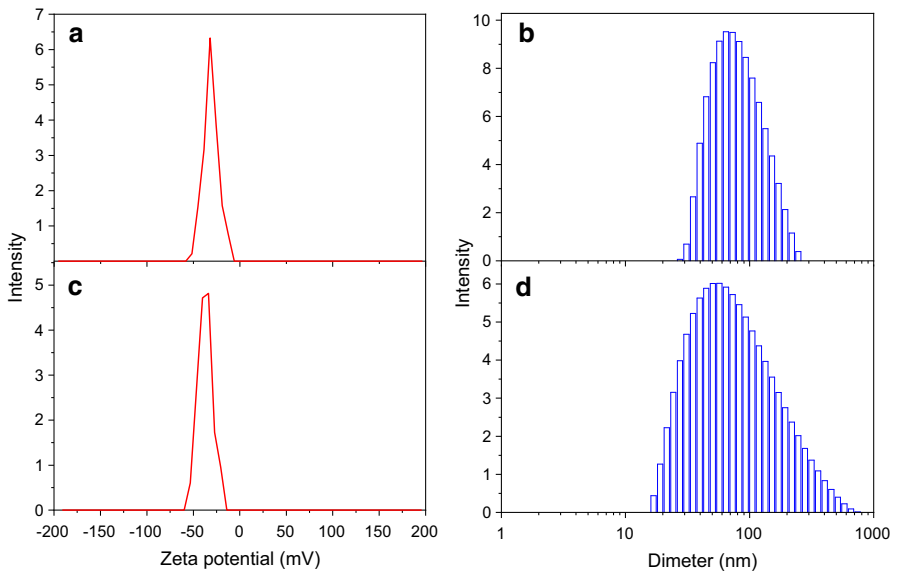
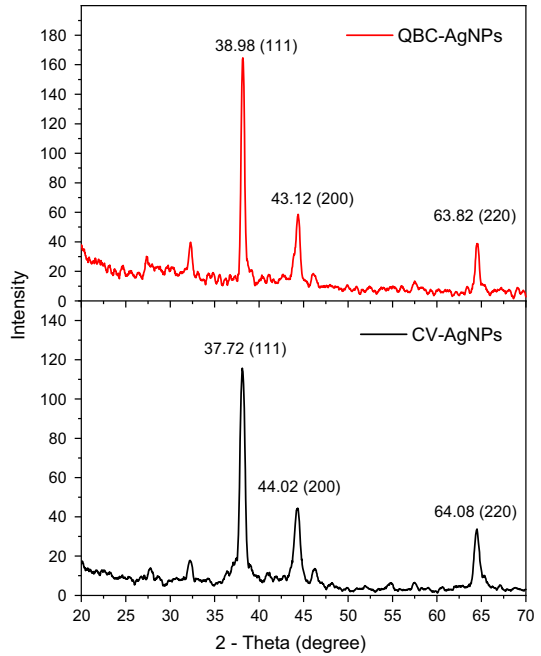


**Fig. 7** DLS spectra (left) and zeta potential (right) of QBC-AgNPs (a and b) and CV-AgNPs (c and d)

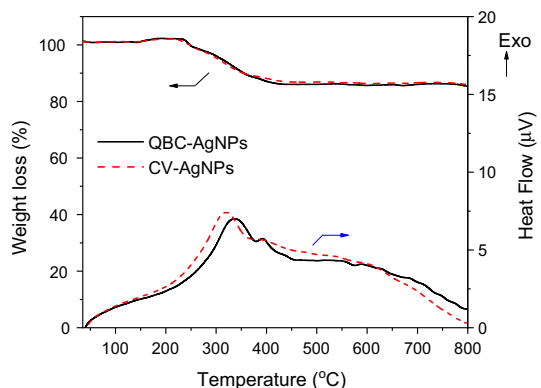
## Thermal behaviors

The percent purity and thermal stability of the biogenic AgNPs were determined by simultaneous TG–DTA analysis. Figure 8 illustrates the TG–DTA curves of AgNPs synthesized by Quao Binh Chau and Che Vang extracts. The mass loss at low temperature (below 200 °C) is not observed in all samples, indicated moisture/solvent absent in the nanoparticles. The total weight loss of two nanoparticles is about 17.0% in temperature range of 220–430 °C that is attributed to content of decomposed biomolecules surrounding the metallic core. DTA curves of QBC-AgNPs and CV-AgNPs showed that oxidation reactions occur at exothermic peaks at 315 and 345 °C, respectively.

## Antibacterial assay

In the present work, the antibacterial activity of the synthesized AgNPs was explored against bacteria including *B. subtilis*, *S. aureus*, *E. coli* and *A. tumefaciens* at the different weights of the sample. Luria–Bertani broth and standard antibiotic ampicillin were utilized as the negative and positive controls, respectively. For all samples, the activity was tested on separate plates against each bacterial strain. The leaf extracts tested at concentration of 10  $\mu\text{L}$  did not inhibit any bacterial strain. The high antibacterial effect was observed in Figures S4 and S5. The zone of inhibition was plotted at varied concentration of the AgNPs and is described in Fig. 9. Both the biosynthesized AgNPs exhibit strong antibacterial activity against all the tested strains. The activity was enhanced with increasing dose concentrations of the samples. Between them, QBC-AgNPs possessed higher activity in inhibition of the strains except *E. coli*. The difference between two nanoparticles can relate to changes in size, morphology and stabilized biomolecules of AgNPs, while different inhibition activity among the bacterial strains can correlate to antibacterial mechanism which depends on the cell walls and cell membrane generation via hydrophobic and bioaccumulation mechanism [44]. Therefore, this study suggests that Quao Binh Chau extract-mediated AgNPs can be used for inhibition of three bacterial strains *B. subtilis*, *S. aureus* and *A. tumefaciens*, while CV-AgNPs should be utilized to inhibit *E. coli*.

**Fig. 8** Simultaneous TG and DTA curves of QBC-AgNPs and CV-AgNPs in air flow of 20 mL/min at heating rate of 10 °C/min



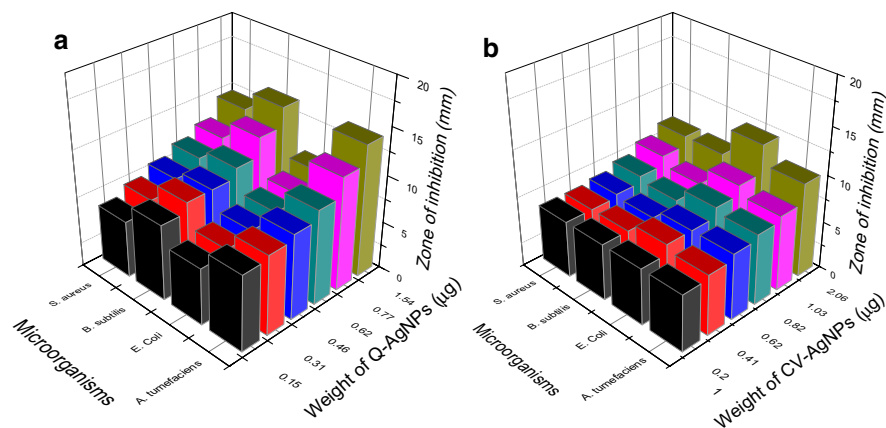


**Fig. 9** Plot zone of inhibition (%) of various bacteria at the different concentrations of QBC-AgNPs (a) and CV-AgNPs (b)

### Catalytic activity

Treatment of water pollution from dyeing industry is always received great concern. Among the methods, degradation of the pollutants using the reductants like  $\text{NaBH}_4$ ,  $\text{H}_2\text{O}_2$  is frequently reported over recent years. In this work, the catalytic activity of the biosynthesized AgNPs is evaluated through degradation reaction of 4-NP and MO using  $\text{NaBH}_4$  in aqueous medium which is well known as a thermodynamically favorable reaction [45]. However, due to large redox potential difference between donor and acceptor molecules, the kinetic barrier reduces feasibility of this reaction. Thus, the catalyst using noble metal nanoparticles like AgNPs is an efficient solution to overcome this kinetic barrier. In the reaction mechanism, metallic surface plays a critical role as an absorbent of the reactants and electron transfers from the electron donor ( $\text{BH}_4^-$ ) to the electron acceptor (i.e., 4-NP, MO) (Fig. 10) [13, 34].

The degradation of 4-NP and MO was evaluated by decrease of absorption intensity at respective peaks of 400 and 464 nm. UV-Vis absorption spectra of the pollutants in the absence and presence of the biosynthetic AgNPs are shown in Figures S2 and S3. In general, a very weak reduction of the pollutants in the absence of the catalyst is observed. It has been reported in elsewhere [24]. Upon the introduction of the AgNPs, the absorption intensity of the corresponding peaks is reduced rapidly. The spectra show that the degradation of both pollutants is completed in 12 min in the catalysis of QBC-AgNPs and 6 min in the catalysis of CV-AgNPs. For kinetic study, the reduction is assumed to follow pseudo-first-order reaction and rate constant  $k$  can be determined from plots of values  $\ln(A/A_0)$  against the reaction time. Figure 11 shows a linear relationship between the parameters which confirmed a pseudo-first-order reaction for degradation of both pollutants. Between two catalysts, a much higher catalytic activity of CV-AgNPs is observed in both the reactions. The rate constants for degradation of 4-nitrophenol in the presence of QBC-AgNPs and CV-AgNPs are found to be  $4.2 \times 10^{-3} \text{ s}^{-1}$  and  $18.2 \times 10^{-3} \text{ s}^{-1}$ , respectively, while

**Fig. 10** Proposed mechanism of AgNPs catalysis in degradation of 4-nitrophenol and methyl orange by  $\text{NaBH}_4$

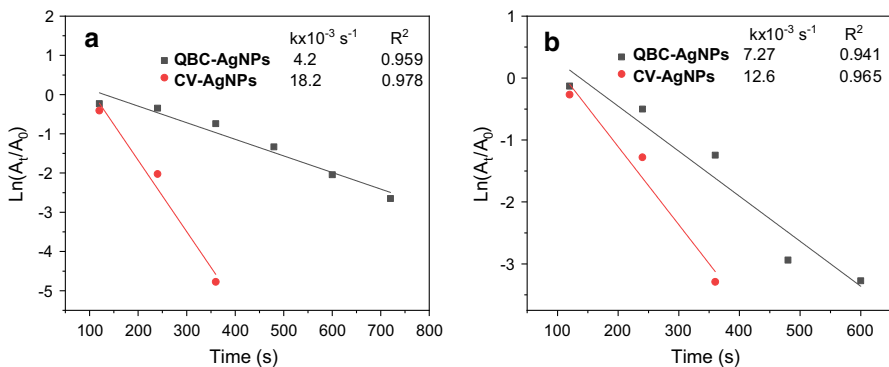
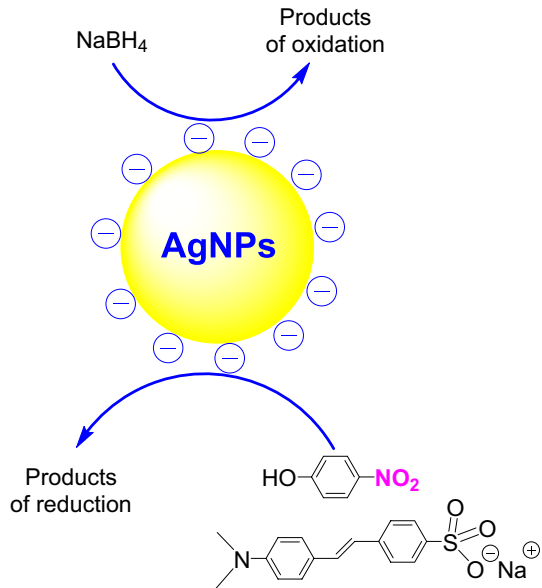


**Fig. 11** First-order kinetics plotted for degradation of 4-nitrophenol (a) and methyl orange (b) in catalysts of QBC-AgNPs and CV-AgNPs

these values for degradation of MO are  $7.3 \times 10^{-3} \text{ s}^{-1}$  and  $12.6 \times 10^{-3} \text{ s}^{-1}$ . The higher catalytic activity of CV-AgNPs can be related to smaller size and consistent distribution of particles which led to a very high surface to volume ratio.

To evaluate catalytic performance of the biosynthesized AgNPs in this work, a comparison with the biogenic AgNPs reported in the literature should be done. The normalized rate constants ( $k_{\text{nor}}$ ) which are defined by rate constants per 1 mg of catalyst are often required [34]. Degradation of 4-NP and MO using the different biogenic AgNPs catalysts is listed in Table 1. The catalysts in this work showed a high performance (2–40 times) in comparison with other works. For example, catalytic activity of CV-AgNPs in the degradation of 4-NPs is 39-fold as much as that

**Table 1** Comparison of the normalized rate constants of biosynthesized AgNPs catalysts for catalytic degradation of 4-nitrophenol and methyl orange

Compd.	Biological system	Size (nm)	$K_{\text{nor}}$ ( $\text{s}^{-1} \text{mg}^{-1}$ )	References
4-NP	<i>Dimocarpus longan</i> seeds	40	$4.7 \times 10^{-4}$	[46]
	<i>Cassia occidentalis</i> leaves	5–25	$1.00 \times 10^{-3}$	[47]
	<i>Arctium lappa</i> root	21.3	$6.77 \times 10^{-3}$	[31]
	<i>Lactuca indica</i> leaves	13.5	$2.1 \times 10^{-3}$	[34]
	<i>Syzygium aromaticum</i> buds	9–15	$2.5 \times 10^{-3}$	[48]
	<i>Stereospermum binhchauensis</i> leaves	20.0	$4.2 \times 10^{-3}$	This work
	<i>Jasminum subtriplinerve</i> leaves	8.0	$18.2 \times 10^{-3}$	This work
MO	<i>Biophytum sensitivum</i> leaves	19–23	$16.2 \times 10^{-3}$	[49]
	<i>Lactuca indica</i> leaves	13.5	$4.37 \times 10^{-3}$	[34]
	<i>Areca catechu</i> nut	18.2–24.3	$4.0 \times 10^{-4}$	[50]
	<i>Arctium lappa</i> root	21.3	$3.70 \times 10^{-3}$	[31]
	<i>Stereospermum binhchauensis</i> leaves	20.0	$7.3 \times 10^{-3}$	This work
	<i>Jasminum subtriplinerve</i> leaves	8.0	$12.6 \times 10^{-3}$	This work

synthesized from *D. longan* seed extract, while this catalyst in the degradation of MO is over 30-fold of activity of AgNPs prepared from *A. catechu* nut. Thus, Quao Binh Chau and Che Vang leaves are an excellent natural material source for production of AgNPs that can efficiently apply in treatment of industrial wastewater.

## Conclusions

The present study described a cost-effective ecofriendly method for the fabrication of multi-functional AgNPs using aqueous extract of *S. binhchauensis* and *J. subtriplinerve* leaves as a natural reducing agent which allows their possible commercial applications. Two principle factors influencing biosynthesis of AgNPs (ratios of silver ions to extract and reaction time) have been optimized based on the UV–Vis method. The high antibacterial activity against four bacterial strains has found for both the biogenic AgNPs. In particular, the AgNPs catalyst showed excellent activity for degradation of toxic compounds by  $\text{NaBH}_4$  in comparison with biogenic AgNPs reported in the literature. Therefore, this work unfolds a high possibility of biogenic AgNPs to be applied as antimicrobial and catalytic agents for environmental technology.

**Acknowledgements** This work is supported by Basic Science Research Fund of Tra Vinh University (No. 168/HD.HDKH-DHTV).

**Data availability** The data used to support the findings of this study are included within the article.

## Compliance with ethical standards

**Conflicts of interest** The authors declare that they have no conflicts of interest.


## References

1. T.A.J.D. Souza, L.R.R. Souza, L.P. Franchi, *Ecotoxicol. Environ. Saf.* **171**, 691 (2019)
2. P. Malik, T.K. Mukherjee, *Int. J. Pharm.* **553**, 483 (2018)
3. A. Loiseau, V. Asila, G. Boitel-Aullen, M. Lam, M. Salmain, S. Boujday, *Biosensors (Basel)* **9**, 78 (2019)
4. N. Sahai, N. Ahmad, M. Gogoi, *Curr. Pathobiol. Rep.* **6**, 219 (2018)
5. S.M. Mousavi, S.A. Hashemi, Y. Ghasemi, A. Atapour, A.M. Amani, A.S. Dashtaki, A. Babapoor, O. Arjmand, *Artif. Cells Nanomed. Biotechnol.* **46**, S855 (2018)
6. M. Jayapriya, D. Dhanasekaran, M. Arulmozhi, E. Nandhakumar, N. Senthilkumar, K. Suresh Kumar, *Res. Chem. Intermediat.* **45**, 3617 (2019)
7. J. Singh, T. Dutta, K.H. Kim, M. Rawat, P. Samddar, P. Kumar, *J. Nanobiotechnol.* **16**, 84 (2018)
8. W.K. Azira, W.M. Khalir, K. Shameli, M. Miyake, N.A. Othman, *Res. Chem. Intermediat.* **44**, 7013 (2018)
9. S. Shah, S. Din, A.K. Rehmanullah, S.A. Shah, *J. Polym. Environ.* **26**, 2323 (2018)
10. P. Khanna, A. Kaur, D. Goyal, *J. Microbiol. Methods* **163**, 105656 (2019)
11. X. Li, H. Xu, Z.S. Chen, G. Chen, *J. Nanomater.* **2011**, 270974 (2011)
12. V. Patel, D. Berthold, P. Puranik, M. Gantar, *Biotechnol. Rep.* **5**, 112 (2015)
13. T.D. Nguyen, T.T. Vo, C.H. Nguyen, V.D. Doan, C.H. Dang, *J. Mol. Liq.* **276**, 927 (2019)
14. R. Arunachalam, S. Dhanasingh, B. Kalimuthu, M. Uthirappan, C. Rose, A.B. Mandal, *Colloids Surf. B* **94**, 226 (2012)
15. A.J. Ruiz-Baltazar, S.Y. Reyes-López, M.L. Mondragón-Sánchez, M. Estevez, A.R. Hernández-Martínez, R. Perez, *Results Phys.* **11**, 1142 (2018)
16. J.L. Lopez-Miranda, M.A.V. González, F. Mares-Briones, J.A. Cervantes-Chávez, R. Esparza, G. Rosas, R. Perez, *Res. Chem. Intermed.* **44**, 7479 (2018)
17. J. Du, Z. Hu, Z. Yu, H. Li, J. Pan, D. Zhao, Y. Bai, *Mater. Sci. Eng. C* **102**, 247 (2019)
18. L. Azeez, A. Lateef, S.A. Adebisi, *Appl. Nanosci.* **7**, 59 (2017)
19. T. Monowar, M.S. Rahman, S.J. Bhore, G. Raju, K.V. Sathasivam, *Molecules* **23**, 3220 (2018)
20. V.S. Dang, *Acta Phytotax. Geobot.* **66**, 91 (2015)
21. N.T.H. Huong, N.K.Q. Cua, T.V. Quy, C.Z. Ganzerac, H. Stuppner, *J. Asian Nat. Prod. Res.* **10**, 1035 (2008)
22. D.T. Mai, T.N. Ngo, N.T.L. Nguyen, Q.L. Ngo, N.P. Minh, T.D. Bui, V.S. Dang, C.L. Tran, N.K.T. Pham, N.M.A. Tran, T.P. Nguyen, *Nat. Prod. Res.* **33**, 1 (2019)
23. D.H. Ngan, H.T.C. Hoai, L.M. Huong, P.E. Hansen, O. Vang, *Nat. Prod. Res.* **22**, 942 (2008)
24. T.D. Nguyen, C.H. Dang, D.T. Mai, *Carbohydr. Polym.* **197**, 29 (2018)
25. M.T. Yagub, T.K. Sen, S. Afroze, H.M. Ang, *Adv. Colloid Interface Sci.* **209**, 172 (2014)
26. B.K.N.N. Ghosh, *J. Nanosci. Nanotechnol.* **18**, 3735 (2018)
27. T.T. Vo, C.H. Dang, V.D. Doan, V.S. Dang, T.D. Nguyen, *J. Inorg. Organomet. Polym. Mater.* **29**, 1 (2019)
28. L. Karimi, S. Zohoori, M.E. Yazdanshenas, *J. Saudi. Chem. Soc.* **18**, 581 (2014)
29. Y. Deng, R. Zhao, *Curr. Pollut. Rep.* **1**, 167 (2015)
30. T.M. Abdelghany, A.M.H. Al-Rajhi, M.A.A. Abboud, M.M. Alawlaqi, A.G. Magdah, E.A.M. Helmy, A.S. Mabrouk, *BioNanoScience* **8**, 5 (2018)
31. T.T.N. Nguyen, T.T. Vo, B.N.H. Nguyen, D.T. Nguyen, V.S. Dang, C.H. Dang, T.D. Nguyen, *Environ. Sci. Pollut. R.* **25**, 34247 (2018)
32. Y. Qin, Y. Liu, L. Yuan, H. Yong, J. Liu, *Food Hydrocoll.* **96**, 102 (2019)
33. C.H. Dang, T.D. Nguyen, *Waste Biomass Valoriz.* **10**, 2703 (2018)
34. T.T. Vo, T.T.N. Nguyen, T.T.T. Huynh, T.T.T. Vo, T.T.N. Nguyen, D.T. Nguyen, V.S. Dang, C.H. Dang, T.D. Nguyen, *J. Nanomater.* **2019**, 8385935 (2019)

35. L.K. Ruddaraju, P.N.V.K. Pallela, S.V.N. Pammi, V.S. Padavala, V.R.M. Kolapalli, *Mat. Sci. Semicond. Proc.* **100**, 301 (2019)
36. A.R. Araujo, J. Ramos-Jesus, T.M. Oliveira, A.M.A.D. Carvalho, P.H.M. Nunes, T.C. Daboit, A.P. Carvalho, M.F. Barroso, M.P. Almeida, A. Plácido, A. Rodrigues, C.C. Portugal, R. Socodato, J.B. Relvas, C. Delerue-Matos, D.A. Silva, P. Eaton, J.R.S.A. Leite, *Ind. Crop Prod.* **137**, 52 (2019)
37. D.Y. Kim, R.G. Saratale, S. Shinde, A. Syed, F. Ameen, G. Ghodake, *J. Clean. Prod.* **172**, 2910 (2018)
38. T.B. Devi, M. Ahmaruzzaman, *Environ. Sci. Pollut. Res.* **23**, 17702 (2016)
39. T. Dodevska, I. Vasileva, P. Denev, D. Karashanova, B. Georgieva, D. Kovacheva, N. Yantcheva, A. Slavov, *Mater. Chem. Phys.* **231**, 335 (2019)
40. S. Islam, B.S. Butola, A. Gupta, A. Roy, *Sustain. Chem. Pharm.* **12**, 100135 (2019)
41. O. Erdogan, M. Abbak, G.M. Demirbolat, F. Birtekocak, M. Aksel, S. Pasa, O. Cevik, *PLoS ONE* **14**, e0216496 (2019)
42. Y.L. Min, G.Q. He, Q.J. Xu, Y.C. Chen, *J. Mater. Chem. A* **2**, 1294 (2014)
43. W.D. Pyrz, D.J. Buttrey, *Langmuir* **24**, 11350 (2008)
44. V. Cittrarasu, B. Balasubramanian, D. Kaliannan, S. Park, V. Maluventhan, T. Kaul, W.C. Liu, M. Arumugam, *Artif. Cells Nanomed. Biotechnol.* **47**, 2424 (2019)
45. V.K. Vidhu, D. Philip, *Micron* **56**, 54 (2014)
46. F.U. Khan, Y. Chen, N.U. Khan, Z.U.H. Khan, A.U. Khan, A. Ahmad, K. Tahir, L. Wang, M.R. Khan, P. Wan, *J. Photochem. Photobiol. B* **164**, 344 (2016)
47. M. Gondwal, G.J.N. Pant, *Int. J. Biomater.* **2018**, 6735426 (2018)
48. B. Ajitha, Y.A.K. Reddy, Y. Lee, M.J. Kim, C.W. Ahn, *Appl. Organomet. Chem.* **33**, e4867 (2019)
49. S. Joseph, B. Mathew, *J. Mol. Liq.* **204**, 184 (2015)
50. A. Rajan, V. Vilas, D. Philip, *J. Mol. Liq.* **207**, 231 (2015)

**Publisher's Note** Springer Nature remains neutral with regard to jurisdictional claims in published maps and institutional affiliations.

## Affiliations

T. My-Thao Nguyen<sup>1</sup> · T. Thanh-Tam Huynh<sup>2,3</sup> · Chi-Hien Dang<sup>3,4</sup> ·  
Dinh-Tri Mai<sup>3,4</sup> · T. Thuy-Nhung Nguyen<sup>5</sup> · Dinh-Truong Nguyen<sup>5</sup> ·  
Van-Su Dang<sup>6</sup> · Trinh-Duy Nguyen<sup>7</sup> · Thanh-Danh Nguyen<sup>2,3</sup> 

<sup>1</sup> Tra Vinh University, Tra Vinh City, Tra Vinh Province, Vietnam

<sup>2</sup> Institute of Research and Development, Duy Tan University, Da Nang City, Vietnam

<sup>3</sup> Institute of Chemical Technology, Vietnam Academy of Science and Technology, 1 Mac Dinh Chi Street, District 1, Ho Chi Minh City, Vietnam

<sup>4</sup> Graduate University of Science and Technology, Vietnam Academy of Science and Technology, 18 Hoang Quoc Viet, Cau Giay District, Hanoi, Vietnam

<sup>5</sup> School of Biotechnology, Tan Tao University, Tan Tao E. City, Long an Province, Vietnam

<sup>6</sup> Department of Chemical Technology, Ho Chi Minh City University of Food Industry, Ho Chi Minh, Vietnam

<sup>7</sup> Center of Excellence for Green Energy and Environmental Nanomaterials, Nguyen Tat Thanh University, Ho Chi Minh City 755414, Vietnam